The Bremmer series for a multi-dimensional acoustic scattering problem

2000 J. Phys. A: Math. Gen. 33 1921

(http://iopscience.iop.org/0305-4470/33/9/314)

J. Phys. A: Math. Gen. **33** (2000) 1921–1932. Printed in the UK PII: S0305-4470(00)04812-5

The Bremmer series for a multi-dimensional acoustic scattering problem

Mats Gustafsson

Department of Electromagnetic Theory, Lund Institute of Technology, Lund University, Box 118 S-221 00 Lund, Sweden

E-mail: mats@teorel.lth.se

Received 27 May 1999, in final form 15 October 1999

Abstract. The Bremmer series is used to reduce a complex scattering problem to a sequence of simpler single-scattering problems. In the Bremmer series, the wave equation is first decomposed into a coupled system of one-way wave equations. The system is then decoupled into a sequence of one-way wave equations with a fixed-point iteration. In this paper, a left-symbol representation of the decomposition operator and the vertical-propagation operator are used. Time-domain convergence of the Bremmer series is shown for a set of dispersive medium models. The non-dispersive case is treated with an approximation procedure.

1. Introduction

We consider a multi-dimensional acoustic scattering problem [3]. An acoustic wave in free space impinges on a region with spatially dependent medium parameters. We use the Bremmer series to transform the problem of the continuously scattered wave into a sequence of simpler scattering problems. Each of the terms in the Bremmer series can be interpreted as the contribution that has been scattered a finite number of times. The Bremmer series approach to a scattering problem starts with a directional decomposition of the wave field into waves propagating in the positive and negative directions. In free space, the decomposition separates the wave equation into two separate one-way wave equations. In a general inhomogeneous medium, the one-way wave equations are coupled via the reflection operator. The Bremmer series decouples the system by a fixed-point iteration.

The advantages and beauty with directional decomposition, or splitting, of waves are best understood in the one-dimensional direct and inverse scattering problems [2, 11]. In multi-dimensions, wave decomposition has been used in a variety of large-scale problems, e.g. exploration seismics, ocean acoustics and fibre optics [17, 20]. In contrast to the one-dimensional case, it is difficult to use an exact wave decomposition in multi-dimensions. Several papers consider the paraxial or beam approximation [10, 13], where the one-way wave operator is approximated with a local operator, asymptotically correct in the preferred direction and in the high-frequency limit. Here, we use a pseudo-differential approximation [5, 10, 15, 17]. This gives a non-local one-way wave operator asymptotically correct in both the high-frequency and high-wavenumber limit. A more careful decomposition is proposed in [6–9].

The Bremmer series was introduced by Bremmer in [2] to solve and analyse a one-dimensional scattering problem. Convergence of the one-dimensional Bremmer series is

0305-4470/00/091921+12$30.00

considered in numerous papers, see e.g. [1, 14]. The series converges in the Fourier domain for sufficiently small and smooth parameters and in general in the time domain. In multi-dimensions, Corones [4] considered the Bremmer series as a correction to the paraxial approximation; the corresponding frequency-domain convergence is analysed in [18]. In [5] de Hoop used pseudo-differential calculus to define and show convergence of the Bremmer series in the Laplace domain for the special case of real values of the Laplace parameter; see also [20].

A typical area of application for the decomposition of waves and the Bremmer series is exploration geophysics. A typical marine survey uses an air gun as a source. The air gun has a power spectrum ranging up to a few kHz and has rather low energy. In this frequency and energy range, the elastic wave propagation in solids is reasonably well described with the non-dispersive acoustic wave equation. To get a more accurate description in a larger frequency range, it is vital to include dispersive properties. In principle, it is not difficult to compute the scattered field, e.g. with a finite difference time-domain scheme [19]. The practical problem is the large-scale structure of the problem that makes a finite difference time-domain computation unfeasible. Instead, it is common to use a temporal Fourier transform followed by a wave decomposition and migration. The Fourier transform calls for the use of parallel computations, and the relatively few frequency components compared with the number of time steps reduce the computations further. Also, observe that there are no complications in including dispersive effects in the algorithm.

In this paper, we use left symbols, see [12], to represent the operators used in the decomposition of the wave field and in the dynamics of the one-way wave equation. The symbols give well-behaved pseudo-differential operators if the Laplace parameter, s, is restricted such that $\operatorname{Re} s \geqslant \alpha|\operatorname{Im} s|$ for some $\alpha \geqslant \alpha_0 > 0$. To get a good time-domain convergence it is important to consider more general values for the Laplace parameter, e.g. $\operatorname{Re} s \geqslant \eta_0$. To accomplish this, we consider passive medium models that reduce to the free-space model in the high-frequency limit. For this model, we show that the Bremmer series converges in the time domain and explicit error estimates are given. The non-dispersive case is treated with an approximation procedure and a weaker time-domain convergence where the field is smoothed by a mollifier.

We follow 'standard' PDE notations as much as possible. Vectors in the Euclidean space $\mathbb{R}^3$ are denoted with a bold face, i.e. $\boldsymbol{x} = (x_1, x_2, x_3) = (x, x_3)$. The vertical direction x_3 is the preferred direction and $x = (x_1, x_2)$ are the transverse directions. The gradient and divergence operators in $\mathbb{R}^3$ are denoted ∇ and $\nabla\cdot$, respectively. For the corresponding transverse part, we use the operator $\mathrm{D} = (\partial_1, \partial_2)$. The norm $\|\cdot\|$ is the usual L^2 norm in $\mathbb{R}^2$, i.e. $\|u\| = \int_{\mathbb{R}^2} |u(x)|^2 \,\mathrm{d}x$. The corresponding norm in $\mathbb{R}^3$ is denoted by $\|\cdot\|_3$. Furthermore, we suppress the coordinate dependence in many expressions, in particular, the dependence of x_3 is often ignored.

2. Acoustic scattering

We consider the acoustic scattering problem depicted in figure 1. An acoustic wave field is generated by the sources, $\boldsymbol{f}(\boldsymbol{x}, t)$ and $q(\boldsymbol{x}, t)$. The induced field is scattered by the medium inhomogeneities. We assume that both the sources and the inhomogeneities vanish outside some compact region. The region outside the slab $0 \leqslant x_3 \leqslant X_3$ is free space; see figure 1. For simplicity, we also assume that there are no sources inside the slab.

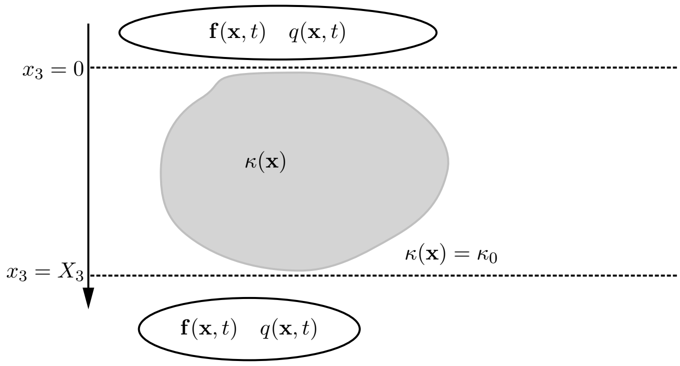

Figure 1. The acoustic scattering geometry.

The acoustic wave equation

$$\begin{aligned} &\partial_t[\kappa p](\boldsymbol{x},t) + \nabla\cdot \boldsymbol{v}(\boldsymbol{x},t) = q(\boldsymbol{x},t) \\ &\rho\partial_t \boldsymbol{v}(\boldsymbol{x},t) + \nabla p(\boldsymbol{x},t) = \boldsymbol{f}(\boldsymbol{x},t) \end{aligned} \tag{1}$$

models the evolution of the fields. The acoustic pressure is denoted by $p(\boldsymbol{x},t)$ and $\boldsymbol{v}(\boldsymbol{x},t)$ is the particle velocity. The medium properties are described by the compressibility κ and the density ρ. The compressibility is temporally dispersive and spatially dependent, whereas the density is assumed to be constant: $\rho = \rho_0$. The temporal dispersion is defined in the Laplace plane (6), (8), and (9). In the scattering problem, we assume that the sources are quiescent and that the fields vanish before time $t = 0$. This gives the initial conditions

$$p(\boldsymbol{x},0) = 0 \qquad \text{and} \qquad \boldsymbol{v}(\boldsymbol{x},0) = \mathbf{0} \tag{2}$$

to the acoustic wave equation (1).

In this paper, we describe a method to solve the acoustic scattering problem (1) in an iterative way—the Bremmer series. Let p and $\boldsymbol{v}$ be the solution of (1). We want to find approximations $\sum p^{(k)}$ and $\sum \boldsymbol{v}^{(k)}$ of p and $\boldsymbol{v}$, respectively, such that

$$\begin{aligned} &\int_{t=0}^{T}\int_{x_3=0}^{X_3} \kappa_0 \left\| \sum_{k=1}^{N} p^{(k)}(\cdot,x_3,t) - p(\cdot,x_3,t)\right\|^2 \\ &\qquad +\rho_0 \left\| \sum_{k=1}^{N} \boldsymbol{v}^{(k)}(\cdot,x_3,t) - \boldsymbol{v}(\cdot,x_3,t)\right\|^2 \mathrm{d}x_3\,\mathrm{d}t \to 0 \qquad \text{as} \quad N\to\infty \end{aligned} \tag{3}$$

for finite times T.

Most of the analysis is performed in the Laplace domain. The Laplace transformed wave-field quantities are denoted with a hat $\hat{\cdot}$, i.e.

$$\hat{p}(\boldsymbol{x},s) = \int_{t=0^-}^{\infty} \mathrm{e}^{-st} p(\boldsymbol{x},t)\,\mathrm{d}t \tag{4}$$

where the Laplace transform parameter s is restricted to a right half-plane $s = \eta + \mathrm{i}\omega$, with $\eta \geqslant 0$. The time-domain wave-field quantities are recovered by the inverse Laplace transform

$$p(\boldsymbol{x},t) = \frac{1}{2\pi}\int_{\omega=-\infty}^{\infty} \mathrm{e}^{(\eta+\mathrm{i}\omega)t}\hat{p}(\boldsymbol{x},\eta+\mathrm{i}\omega)\,\mathrm{d}\omega. \tag{5}$$

The Laplace-transformed version of the acoustic equation (1) is

$$\begin{aligned} &s\kappa(\boldsymbol{x},s)\hat{p}(\boldsymbol{x},s) + \nabla\cdot\hat{\boldsymbol{v}}(\boldsymbol{x},s) = \hat{q}(\boldsymbol{x},s) \\ &s\rho\hat{\boldsymbol{v}}(\boldsymbol{x},s) + \nabla\hat{p}(\boldsymbol{x},s) = \hat{\boldsymbol{f}}(\boldsymbol{x},s) \end{aligned} \tag{6}$$

together with the radiation condition

$$\sqrt{\rho_0}\hat{v}_r - \sqrt{\kappa_0}\hat{p} = \mathrm{o}(|\boldsymbol{x}|^{-1}) = \mathrm{o}(r^{-1}) \tag{7}$$

where $\hat{v}_r$ stands for the radial component of the particle velocity. To ensure causality the compressibility $\kappa(\boldsymbol{x}, s)$ is an analytic function of s in the right complex half-plane. Furthermore, we restrict the analysis to passive dispersive models such that

$$\mathrm{Re}\,\{s\kappa(\boldsymbol{x}, s)\} \geqslant \kappa_0\eta \tag{8}$$

and

$$\kappa(\boldsymbol{x}, s) - \kappa_0 = \mathrm{O}(s^{-2}) \qquad \text{as} \quad s \to \infty. \tag{9}$$

For simplicity, we assume that $\kappa(\boldsymbol{x}, s)$ depends smoothly on the spatial coordinate $\boldsymbol{x}$. It is convenient to write the compressibility (9) as a perturbation of free space, i.e.

$$\kappa(\boldsymbol{x}, s) = \kappa_0 + \delta\psi(\boldsymbol{x}, s)s^{-2} \tag{10}$$

where $\psi(\boldsymbol{x}, s)$ is uniformly bounded in $\boldsymbol{x}$ and s for $\mathrm{Re}\, s \geqslant \beta_0 > 0$. The parameter δ is used to denote the size of the perturbation. Observe that the first-order system (6) corresponds to a dispersive velocity model for the second-order wave equation.

3. Non-dispersive medium

We also consider the non-dispersive model

$$\kappa(\boldsymbol{x}, s) = \kappa(\boldsymbol{x}) \tag{11}$$

i.e. the compressibility κ depends on the spatial coordinates $\boldsymbol{x}$, but not on the Laplace parameter s. The compressibility is assumed to be smooth and uniformly bounded, i.e. $0 < \kappa_0 \leqslant \kappa(\boldsymbol{x}) \leqslant \kappa_1$. Outside some compact region it reduces to the free-space value κ_0. The density is assumed to be constant, $\rho = \rho_0$ everywhere. We introduce a dispersive model (8) and (9) that resembles the non-dispersive model (11) for low frequencies. The model is given by

$$\kappa_{\omega_0}(\boldsymbol{x}, s) = \kappa_0 + \frac{(\kappa(\boldsymbol{x}) - \kappa_0)\omega_0^2}{\omega_0^2 + s^2} = \kappa(\boldsymbol{x}) - \frac{(\kappa(\boldsymbol{x}) - \kappa_0)s^2}{\omega_0^2 + s^2}. \tag{12}$$

Observe that (12) is a mathematical construction and not an attempt to model actual processes in the medium. This model satisfies conditions (8) and (9). The advantage with the dispersive model is that it removes the spatial dependence in the principal part of the equation, and hence simplifies the analysis.

For low frequencies, $|s| \ll \omega_0$, the dispersive model (12) is a good approximation to the non-dispersive model (11) and the corresponding error in the solution to the acoustic equation (6) is small; see the appendix. However, we cannot expect the error to be small in the time domain, i.e. the high-frequency part of the constitutive relations (11) and (12) are different and hence the wavefront set of the time-domain solution will be different. To overcome this problem, we introduce a smoothed or frequency-filtered version of the time-domain fields $p(t)$ and $\boldsymbol{v}(t)$ defined as

$$\tilde{p}(t) = \int_0^t p(t - t')\chi_\tau(t')\,\mathrm{d}t' = (p * \chi_\tau)(t) = \frac{1}{2\pi}\int_{\eta-\mathrm{i}\infty}^{\eta+\mathrm{i}\infty} \mathrm{e}^{st}\hat{p}(s)\hat{\chi}_\tau(s)\,\mathrm{d}\omega \tag{13}$$

where $\hat{\chi}_\tau(s)$ is a suitable weight function and $\hat{p}$ is the solution of the acoustic equation, (6), with the radiation condition, (7). The smoothed velocity field $\tilde{\boldsymbol{v}}(t)$ is defined in an analogous fashion. The weight function $\chi_\tau(t)$ is a smooth, positive, and causal function with unit integral and supported in $[0, \tau]$, i.e. a mollifier. The Laplace-transformed version of the weight function $\hat{\chi}_\tau(s)$ is analytic for $\mathrm{Re}\, s > 0$ and decays exponentially, i.e. there are numbers C_M such that

$$|\hat{\chi}_\tau(s)| \leqslant C_M(1 + |s|)^{-M} \qquad \text{for all} \quad M. \tag{14}$$

Observe that the weight function approaches the Dirac delta distribution $\delta(t)$ for small times, i.e. $\chi_\tau(t) \to \delta(t)$ as $\tau \to 0$, and hence the frequency-filtered fields resemble the original fields for small times τ.

For the non-dispersive medium, we show that the sum of the frequency-filtered Bremmer series fields $\tilde{p}^{(k)}_{\omega_0}$ and $\tilde{\boldsymbol{v}}^{(k)}_{\omega_0}$ converge to the original frequency-filtered fields $\tilde{p}$ and $\tilde{\boldsymbol{v}}$ as the number of Bremmer terms increase and $\omega_0 \to \infty$. It is advantageous to show the convergence in two steps. First, we let the Bremmer iteration limit $N \to \infty$, and then separately, the frequency limit $\omega_0 \to \infty$. Let $\hat{p}_{\omega_0}$ and $\hat{\boldsymbol{v}}_{\omega_0}$ be the solution to (6) with the approximate compressibility (12). Assuming that the Bremmer iteration (3) converges, then

$$\sum_{k=1}^{N} p^{(k)}_{\omega_0} \to p_{\omega_0} \qquad \text{and} \qquad \sum_{k=1}^{N} \boldsymbol{v}^{(k)}_{\omega_0} \to \boldsymbol{v}_{\omega_0} \qquad \text{as} \quad N \to \infty \tag{15}$$

and according to (61)

$$\tilde{p}_{\omega_0} \to \tilde{p} \qquad \text{and} \qquad \tilde{\boldsymbol{v}}_{\omega_0} \to \tilde{\boldsymbol{v}} \qquad \text{as} \quad \omega_0 \to \infty. \tag{16}$$

So in total, we have convergence. However, observe that the constants in the dispersive approximation (12) increase with ω_0 and hence the convergence properties of the Bremmer series deteriorate.

4. Approximate wave decomposition

The acoustic wave equation (1) is usually solved by a time-stepping procedure. However, this is computationally inefficient for large problems. In order to get a more numerically efficient solution, we decompose the acoustic wave equation into its up- and down-going parts [5].

Write the Laplace-transformed system (6) as a formal evolution problem in the preferred direction x_3

$$(\partial_3 + \mathcal{A})\hat{w} = \hat{g}. \tag{17}$$

The system matrix $\mathcal{A}$ is

$$\mathcal{A} = \begin{pmatrix} 0 & s\rho \\ -\mathrm{D}\cdot(s^{-1}\rho^{-1}\mathrm{D}) + s\kappa(x, x_3, s) & 0 \end{pmatrix} \tag{18}$$

and the field vector $\hat{w}$ and source vector $\hat{g}$ are

$$\hat{w} = \begin{pmatrix} \hat{p} \\ \hat{v}_3 \end{pmatrix} \qquad \text{and} \qquad \hat{g} = \begin{pmatrix} \hat{f}_3 \\ \hat{q} + \mathrm{D}\cdot(\rho^{-1}s^{-1}\hat{f}) \end{pmatrix} \tag{19}$$

respectively. Problem (17) is not well posed for marching in the x_3 direction, but it is possible to decompose system (17) into two parts, one propagating in the positive x_3 direction and the other in the negative x_3 direction. We decompose the system by formally diagonalizing the system matrix (18). The diagonalization operator is only determined up to a normalization; here we use the acoustic-pressure normalization [5]. The diagonal elements are the square root of the characteristic operator

$$\begin{aligned} \mathrm{A} &= -\partial_1^2 - \partial_2^2 + s^2\kappa(x, x_3, s)\rho = -\mathrm{D}^2 + s^2c^{-2}(x, x_3, s) \\ &= -\mathrm{D}^2 + s^2c_0^{-2} + \delta\psi(x, x_3, s). \end{aligned} \tag{20}$$

In general, it is difficult to define an exact square root, so instead we determine an approximate square root of A. Let Γ be an operator such that the difference $\mathrm{A} - \Gamma^2$ is small. We call Γ the vertical-propagation operator for the acoustic wave equation. Let Ξ denote the error in the approximation of the square-root operator, i.e.

$$\Xi = (\Gamma - \Gamma^{-1}\mathrm{A})/2. \tag{21}$$

We construct approximations of $\mathrm{A}^{1/2}$, such that Ξ is small in a general medium and vanishes identically in a homogeneous medium. In the acoustic-pressure normalization, the composition operator L and the decomposition operator L^{-1} are defined as

$$\mathrm{L} = \begin{pmatrix} \rho & \rho \\ s^{-1}\Gamma & -s^{-1}\Gamma \end{pmatrix} \qquad \text{and} \qquad \mathrm{L}^{-1} = \frac{1}{2}\begin{pmatrix} \rho^{-1} & s\Gamma^{-1} \\ \rho^{-1} & -s\Gamma^{-1} \end{pmatrix} \tag{22}$$

respectively. The decomposition operator L^{-1} defines the down- and up-going components $\hat{u} = (\hat{u}_+, \hat{u}_-)^{\mathrm{T}}$ of the wave field, see figure 2. We substitute $\hat{w} = \mathrm{L}\hat{u}$ into the dynamics (17) to get

$$(\partial_3\mathrm{L} + \mathcal{A}\mathrm{L})\hat{u} = \hat{g}. \tag{23}$$

Next we multiply with the decomposition operator and use the relation $\partial_3\mathrm{L} = (\partial_3\mathrm{L}) + \mathrm{L}\partial_3$. This gives

$$(\partial_3 + \mathrm{L}^{-1}\mathcal{A}\mathrm{L})\hat{u} = -\mathrm{L}^{-1}(\partial_3\mathrm{L})\hat{u} + \mathrm{L}^{-1}\hat{g}. \tag{24}$$

The principal part of the equation decouples

$$\mathrm{L}^{-1}\mathcal{A}\mathrm{L} = \frac{1}{2}\begin{pmatrix} \Gamma + \Gamma^{-1}\mathrm{A} & -\Gamma + \Gamma^{-1}\mathrm{A} \\ \Gamma - \Gamma^{-1}\mathrm{A} & -\Gamma - \Gamma^{-1}\mathrm{A} \end{pmatrix} = \begin{pmatrix} \Gamma & 0 \\ 0 & -\Gamma \end{pmatrix} + \begin{pmatrix} -\Xi & -\Xi \\ \Xi & \Xi \end{pmatrix} \tag{25}$$

if Ξ is of lower order than Γ. In the region $0 \leqslant x_3 \leqslant X_3$, the decomposed fields $\hat{u}$ satisfy the source-free one-way system of equations

$$\begin{pmatrix} \partial_3 + \Gamma & 0 \\ 0 & \partial_3 - \Gamma \end{pmatrix}\begin{pmatrix} \hat{u}_+ \\ \hat{u}_- \end{pmatrix} = \begin{pmatrix} \mathrm{R}_{1,1} & \mathrm{R}_{1,2} \\ \mathrm{R}_{2,1} & \mathrm{R}_{2,2} \end{pmatrix}\begin{pmatrix} \hat{u}_+ \\ \hat{u}_- \end{pmatrix} \tag{26}$$

where the matrix-valued interaction operator $\mathcal{R}$ is

$$\mathcal{R} = \begin{pmatrix} \mathrm{R}_{1,1} & \mathrm{R}_{1,2} \\ \mathrm{R}_{2,1} & \mathrm{R}_{2,2} \end{pmatrix} = \Gamma^{-1}\partial_3\Gamma/2\begin{pmatrix} 1 & -1 \\ -1 & 1 \end{pmatrix} + \Xi\begin{pmatrix} 1 & 1 \\ -1 & -1 \end{pmatrix}. \tag{27}$$

Notice that the first part of the interaction operator reduce to the classical reflection operator for a layered media, i.e.

$$\mathrm{R} = \Gamma^{-1}\partial_3\Gamma/2 = (\Gamma_a + \Gamma_b)^{-1}(\Gamma_a - \Gamma_b) \tag{28}$$

where Γ_a and Γ_b are the vertical-propagation operators in two adjacent layers. The boundary conditions for the one-way wave system of equations (26) are

$$\hat{u}_+(x, 0) = \hat{u}_+^{(0)}(x) \qquad \text{and} \qquad \hat{u}_-(x, X_3) = \hat{u}_-^{(0)}(x) \tag{29}$$

where the boundary terms are obtained from the solution of the one-way problem (26) in free space. In free space, the vertical-propagation operator Γ reduces to multiplication with the free space vertical-propagation symbol

$$\gamma_0(\xi, s) = \sqrt{c_0^{-2}s^2 + \xi^2} \tag{30}$$

in the spatial Fourier domain, i.e.

$$\Gamma_0\hat{u}(x) = (2\pi)^{-2}\int_{y\in\mathbb{R}^2}\int_{\xi\in\mathbb{R}^2}\gamma_0(\xi, s)\mathrm{e}^{\mathrm{i}\xi\cdot(x-y)}\hat{u}(y)\,\mathrm{d}y\,\mathrm{d}\xi. \tag{31}$$

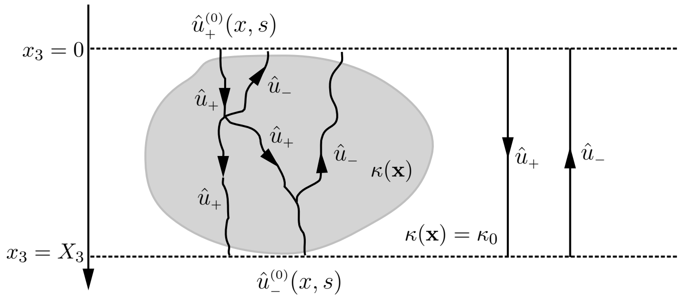

Figure 2. The one-way acoustic scattering geometry.

The solution is

$$\hat{u}_+^{(0)}(x) = (2\pi)^{-2} \int_{x_3=-\infty}^{0} \int_{\xi\in\mathbb{R}^2} \int_{y\in\mathbb{R}^2} \mathrm{e}^{\mathrm{i}\xi\cdot(x-y)} \mathrm{e}^{\gamma_0 x_3} \hat{g}_+(y, x_3)\, \mathrm{d}y\, \mathrm{d}\xi\, \mathrm{d}x_3$$

$$\hat{u}_-^{(0)}(x) = (2\pi)^{-2} \int_{x_3=X_3}^{\infty} \int_{\xi\in\mathbb{R}^2} \int_{y\in\mathbb{R}^2} \mathrm{e}^{\mathrm{i}\xi\cdot(x-y)} \mathrm{e}^{-\gamma_0 x_3} \hat{g}_-(y, x_3)\, \mathrm{d}y\, \mathrm{d}\xi\, \mathrm{d}x_3$$

where $\hat{g}_+$ and $\hat{g}_-$ are the down- and up-going parts of the source, i.e.

$$\hat{g}_+ = (\rho^{-1}\hat{g}_1 + s\Gamma_0^{-1}\hat{g}_2)/2 \qquad \text{and} \qquad \hat{g}_- = (\rho^{-1}\hat{g}_1 - s\Gamma_0^{-1}\hat{g}_2)/2 \tag{32}$$

respectively.

5. The vertical-propagation operator

The vertical-propagation operator Γ can be represented in a variety of ways, e.g. left-, right-, Weyl-symbols and spectral theory; see [5,7,9]. Here, we use a left-symbol representation, i.e., the operator is defined as the action of the integral

$$(\Gamma\hat{u})(x, s) = (2\pi)^{-2} \int_{\xi\in\mathbb{R}^2} \int_{y\in\mathbb{R}^2} \gamma(x, \xi, s) \mathrm{e}^{\mathrm{i}(x-y)\cdot\xi} \hat{u}(y, s)\, \mathrm{d}y\, \mathrm{d}\xi \tag{33}$$

where $\gamma(x, \xi, s)$ is the vertical-propagation symbol (or coefficient)

$$\gamma(x, \xi, s) = \sqrt{c^{-2}(x, s)s^2 + \xi^2} = \sqrt{c_0^{-2}s^2 + \xi^2 + \delta\psi(x, s)}. \tag{34}$$

We use the dispersive property (9) to analyse Γ and to get uniform estimates of Γ for s in a half-plane $\mathrm{Re}\, s \geqslant \eta_0 > 0$.

We start with some properties of the free-space vertical-propagation operator, Γ_0, defined in (31). The real-valued part of s is a lower bound of the real-valued part of γ_0, i.e. $\mathrm{Re}\,\gamma \geqslant c_0^{-1}\eta$. Fourier calculus give a similar lower bound on the symmetric part of the free space vertical-propagation operator

$$\mathrm{Re}\,\Gamma_0 \geqslant c_0^{-1}\eta \tag{35}$$

and an upper bound on the inverse

$$\|\Gamma_0^{-1}\| \leqslant c_0\eta^{-1}. \tag{36}$$

We expand the vertical-propagation operator Γ in the free space vertical-propagation operator Γ_0. Extract the free space symbol from the symbol (34)

$$\gamma(x, \xi, s) = \gamma_0(\xi, s)\sqrt{1 + \delta\gamma_0^{-2}(\xi, s)\psi(x, s)}. \tag{37}$$

The symbol ψ contains all inhomogeneous and dispersive parts and it is uniformly bounded in x, x_3, and s. For sufficiently large values of η, we can expand the symbol in the binomial series

$$\gamma(x,\xi,s) = \gamma_0(\xi,s) + \sum_{n=1}^{\infty} \binom{\frac{1}{2}}{n} \delta^n \psi^n(x,s)\gamma_0^{1-2n}(\xi,s). \tag{38}$$

Use the linearity of the left symbol and the left-symbol composition rule

$$(\Psi\Gamma_0\hat{u})(x,s) = (2\pi)^{-2}\int_{\xi\in\mathbb{R}^2}\int_{y\in\mathbb{R}^2} \mathrm{e}^{\mathrm{i}\xi\cdot(x-y)}\psi(x,s)\gamma_0(\xi,s)\hat{u}(y)\,\mathrm{d}y\,\mathrm{d}\xi \tag{39}$$

where Ψ is the multiplicative operator associated with the symbol ψ, i.e. $\Psi = \psi$. The vertical-propagation operator is

$$\Gamma = \Gamma_0 + \sum_{n=1}^{\infty} \binom{\frac{1}{2}}{n} \delta^n \Psi^n \Gamma_0^{1-2n} = \Gamma_0 + \frac{\delta}{2}\Psi\Gamma_0^{-1} + \mathrm{O}(\delta^2/\eta^3) \tag{40}$$

where $\mathrm{O}(\delta^k/\eta^l)$ denotes an operator of the size $\delta^k\Psi^k\Gamma_0^{-l}$, i.e. there is a constant C' such that

$$\|\mathrm{O}(\delta^k/\eta^l)\| \leqslant C'\delta^k\eta^{-l}. \tag{41}$$

Use (40) and the coercivity, (35), to get the estimate

$$\mathrm{Re}\,\Gamma \geqslant c_0^{-1}\eta/2 \tag{42}$$

for sufficiently large values of η. The inverse of the vertical-propagation operator Γ^{-1} is

$$\begin{aligned}\Gamma^{-1} &= (1 + \Gamma_0^{-1}\Psi\Gamma_0^{-1}\delta/2 + \mathrm{O}(\delta^2/\eta^4))^{-1}\Gamma_0^{-1} \\ &= \Gamma_0^{-1} - \Gamma_0^{-1}\Psi\Gamma_0^{-2}\delta/2 + \mathrm{O}(\delta^2/\eta^5).\end{aligned} \tag{43}$$

Notice that the vertical-propagation operator is a perturbation of the free space vertical-propagation operator, i.e. $\Gamma \sim \Gamma_0$ for large η.

The representations (40) and (43) are used to derive uniform estimates on the operators in section 4. The error term Ξ of the square-root approximation (21) is

$$\Xi = (\Gamma - \Gamma^{-1}\mathrm{A})/2 = \delta(\Psi\Gamma_0^{-1} - \Gamma_0^{-1}\Psi)/4 + \mathrm{O}(\delta^2/\eta^3). \tag{44}$$

The reflection operator (27) is estimated as

$$\begin{aligned}\Gamma^{-1}\partial_3\Gamma &= (\Gamma_0^{-1} - \Gamma_0^{-1}\Psi\Gamma_0^{-2}\delta/2 + \mathrm{O}(\delta^2/\eta^4))(\partial_3\Psi\Gamma_0\delta + \mathrm{O}(\delta^2/\eta^3)) \\ &= \delta\Gamma_0^{-1}\partial_3\Psi\Gamma_0^{-1} + \mathrm{O}(\delta^2/\eta^3).\end{aligned} \tag{45}$$

In total, we get a uniform bound on the interaction operator $\mathcal{R}$, i.e. there is a constant C such that

$$\|\mathcal{R}\| \leqslant C\delta\eta^{-1} \qquad \text{for all } x_3 \text{ and } s \text{ such that } \mathrm{Re}\,s \geqslant \eta_0 \tag{46}$$

with η_0 sufficiently large. Notice that it would be sufficient to use the free space vertical-propagation operator in the approximate wave decomposition to get estimates (42) and (46).

It is interesting to compare the analysis above with the classical pseudo-differential calculus. The vertical-propagation operator Γ is a classical pseudo-differential operator for fixed s. Pseudo-differential calculus can be used to show uniform estimates of the Γ operator provided that the Laplace parameter s is restricted to regions such that $\mathrm{Re}\,s \geqslant \eta_0 + \alpha|\mathrm{Im}\,s|$ for some $\alpha \geqslant \alpha_0 > 0$. Due to the hyperbolic nature of the characteristic operator it is difficult to derive uniform estimates in a half-plane with classical pseudo-differential calculus. In [5], a similar analysis is performed with pseudo-differential calculus to analyse the square-root operator $\mathrm{A}^{1/2}$ for $s = \eta > \eta_0$.

6. Bremmer series

In section 4, we decomposed the scattering problem, (1), into the one-way system, (26), together with the boundary conditions, (29), and in section 5 we used the symbol representation to find *a priori* estimates on the one-way wave operators. In the Bremmer series, we solve the scattering problem (26) in an iterative fashion, i.e. fixed-point iterations, Neumann series or successive approximations. The initial step and the succeeding iterations are

$$\begin{cases} (\partial_3 + \Gamma - \mathrm{R}_{1,1})\hat{u}_+^{(1)} = 0 \\ (\partial_3 - \Gamma - \mathrm{R}_{2,2})\hat{u}_-^{(1)} = 0 \\ \hat{u}_+^{(1)}(x,0) = \hat{u}_+^{(0)}(x) \\ \hat{u}_-^{(1)}(x,X_3) = \hat{u}_-^{(0)}(x) \end{cases} \qquad 0 \leqslant x_3 \leqslant X_3 \tag{47}$$

and

$$\begin{cases} (\partial_3 + \Gamma - \mathrm{R}_{1,1})\hat{u}_+^{(k)} = \mathrm{R}_{1,2}\hat{u}_-^{(k-1)} \\ (\partial_3 - \Gamma - \mathrm{R}_{2,2})\hat{u}_-^{(k)} = \mathrm{R}_{2,1}\hat{u}_+^{(k-1)} \\ \hat{u}_+^{(k)}(x,0) = 0 \\ \hat{u}_-^{(k)}(x,X_3) = 0 \end{cases} \qquad 0 \leqslant x_3 \leqslant X_3 \qquad k = 2, 3, \ldots \tag{48}$$

respectively. The fields outside the strip $[0, X_3]$ are determined with the free-space vertical-propagation operator Γ_0. Observe that there is an ambiguity in the definition of the Bremmer series regarding the position of the transmission part of the interaction operator. In approaches based on integral equations it is common to include the transmission part in the right-hand side of the iteration [5]. Here, we choose to update the fields as much as possible and hence include the transmission part in the left-hand side. The convergence proof is essentially independent of this choice.

The total wave field is the sum of the Bremmer terms in (47) and (48)

$$\hat{u} = \sum_{k=1}^{\infty} \hat{u}^{(k)}. \tag{49}$$

The sequence converges, if the iteration is a contraction. We use energy estimates to get an L^2 bound; see [16]. Equations (48) are multiplied with $\hat{u}_+$ and $\hat{u}_-$, respectively, and the estimates (42) and (46) are used to get

$$\partial_3 \|\hat{u}_+^{(k)}(\cdot, x_3)\|^2 + (\eta c_0^{-1} - 3C\delta\eta^{-1})\|\hat{u}_+^{(k)}(\cdot, x_3)\|^2 \leqslant C\delta\eta^{-1}\|\hat{u}_-^{(k-1)}(\cdot, x_3)\|^2$$
$$-\partial_3 \|\hat{u}_-^{(k)}(\cdot, x_3)\|^2 + (\eta c_0^{-1} - 3C\delta\eta^{-1})\|\hat{u}_-^{(k)}(\cdot, x_3)\|^2 \leqslant C\delta\eta^{-1}\|\hat{u}_+^{(k-1)}(\cdot, x_3)\|^2.$$

Next we integrate the inequalities over $[0, X_3]$. This gives the bounds

$$\begin{aligned} \int_0^{X_3} \|\hat{u}_+^{(k)}(\cdot, x_3)\|^2 \,\mathrm{d}x_3 &\leqslant \frac{C\delta}{\eta^2 c_0^{-1} - 3C\delta} \int_0^{X_3} \|\hat{u}_-^{(k-1)}(\cdot, x_3)\|^2 \,\mathrm{d}x_3 \\ \int_0^{X_3} \|\hat{u}_-^{(k)}(\cdot, x_3)\|^2 \,\mathrm{d}x_3 &\leqslant \frac{C\delta}{\eta^2 c_0^{-1} - 3C\delta} \int_0^{X_3} \|\hat{u}_+^{(k-1)}(\cdot, x_3)\|^2 \,\mathrm{d}x_3. \end{aligned} \tag{50}$$

The final bound is obtained by adding the two inequalities

$$\int_0^{X_3} \|\hat{u}^{(k)}(\cdot, x_3)\|^2 \,\mathrm{d}x_3 \leqslant \frac{C\delta}{\eta^2 c_0^{-1} - 3C\delta} \int_0^{X_3} \|\hat{u}^{(k-1)}(\cdot, x_3)\|^2 \,\mathrm{d}x_3. \tag{51}$$

For η sufficiently large, i.e. $\eta^2 \geqslant 4C\delta c_0$, the map is a contraction and the Bremmer series (48) converges. The initial step in (47) gives, in a similar way, a bound on the first term

$$\int_0^{X_3} \|\hat{u}^{(1)}(\cdot, x_3)\|^2 \,\mathrm{d}x_3 \leqslant \|\hat{u}^{(0)}(\cdot)\|^2 \tag{52}$$

for $\eta^2 \geqslant 4C\delta c_0$.

To show that there exists a solution to the one-way systems (47) and (48), we can use the free-space representations (40), (42), and (43). The one-way system is iterated with the free-space solution (existence of the free-space solution follows from Fourier calculus). The iteration converges for sufficiently large values of η_0.

6.1. Convergence rate

In the Bremmer series, the real-valued part of the Laplace parameter is fixed at the value, $\operatorname{Re} s = \eta$. We iterate the series N times and subsequently go back to the time domain through the inverse Laplace transform (5). If the parameter η is increased the series converge faster. However, the error has to be smaller due to multiplication with $e^{\eta t}$ in the inverse Laplace transformation. For a fixed time $t = T$, the series can be iterated until the error is small enough (assume no numerical truncation errors) and the inverse Laplace transformation gives time-domain convergence.

A rough estimate of the error is

$$\begin{aligned}
&\int_{t=0}^{T}\int_{x_3=0}^{X_3} \left\| \sum_{k=1}^{N} u^{(k)}(\cdot, x_3, t) - u(\cdot, x_3, t)\right\|^2 \mathrm{d}x_3\,\mathrm{d}t \\
&\quad\leqslant \frac{e^{2\eta T}}{2\pi}\int_{\omega=-\infty}^{\infty}\int_{x_3=0}^{X_3} \left\| \sum_{k=1}^{N} \hat{u}^{(k)}(\cdot, x_3, \eta + \mathrm{i}\omega) - \hat{u}(\cdot, x_3, \eta + \mathrm{i}\omega)\right\|^2 \mathrm{d}x_3\,\mathrm{d}\omega \\
&\quad\leqslant e^{2\eta T}\int_{t=0}^{T} \|u^{(0)}(\cdot, t)\|^2\,\mathrm{d}t \sum_{k=N}^{\infty}\left(\frac{C\delta}{\eta^2 c_0^{-1} - 3C\delta}\right)^k.
\end{aligned} \tag{53}$$

The error estimate (53) gives the convergence rate

$$N \sim \eta T - \ln(\mathrm{Error}) \tag{54}$$

for large values of η. The number of iterations grows linearly in time, and the accuracy convergence is of exponential order, see [20] for corresponding numerical results in one spatial dimension. The error can be made arbitrarily small by iterating the series enough number of times.

It is also interesting to consider the asymptotic convergence in weak scattering. Let the compressibility by a small perturbation of free space, i.e., δ is small. We get the asymptotic convergence

$$\int_{t=0}^{T}\int_{x_3=0}^{X_3} \left\| \sum_{k=1}^{N} u^{(k)}(\cdot, x_3, t) - u(\cdot, x_3, t)\right\|^2 \mathrm{d}x_3\,\mathrm{d}t = \mathrm{O}(\delta^N). \tag{55}$$

7. Discussion

In this paper, we have shown that the Bremmer series converges in the time domain for a multi-dimensional dispersive acoustic scattering problem. The analysis is restricted to models with constant density and smooth temporally dispersive compressibility. In many applications it is important to consider non-smooth models, e.g., discontinuous media. To get an efficient numerical implementation it is vital to approximate the vertical-propagation operator further, e.g. the split step, phase screen, and the generalized screen method. This and some other generalizations are under investigation. Here, it is interesting to observe the similarity between the product expansion in (38) and the approximation employed in the generalized screen approximation.

Acknowledgments

I am grateful to Professor Martijn de Hoop at the Center for Wave Phenomena, Colorado School of Mines, USA, and Professor David Wall at the Department of Mathematics and Statistics, Canterbury University, New Zealand for their hospitality, and to 'Crafoordska stiftelsen', The Royal Swedish Academy of Sciences, and 'Kungl. Fysiografiska sällskapet i Lund' for partial financial support during the work. Finally, I would like to acknowledge the valuable discussions with Professor Gerhard Kristensson, Doctor Anders Karlsson, MSc Lars Jonsson, Professor Anders Melin, and Professor Ari Laptev.

Appendix. Energy estimates

We have the following energy identity for the acoustic equation (6):

$$\mathrm{Re}\,\{s\kappa\}|\hat{p}|^2 + \mathrm{Re}\,\{s\rho\}|\hat{\boldsymbol{v}}|^2 + \nabla\cdot\mathrm{Re}\,\{\hat{p}^*\hat{\boldsymbol{v}}\} = \mathrm{Re}\,\{\hat{p}^*\hat{q} + \hat{\boldsymbol{v}}^*\cdot\hat{\boldsymbol{f}}\}. \tag{56}$$

We integrate over $\mathbb{R}^3$ and use the radiation conditions, (7), to get the energy estimate,

$$\kappa_0\|\hat{p}\|_3^2 + \rho_0\|\hat{\boldsymbol{v}}\|_3^2 \leqslant \frac{\kappa_0^{-1}\|\hat{q}\|_3^2 + \rho_0^{-1}\|\hat{\boldsymbol{f}}\|_3^2}{4\epsilon(\eta-\epsilon)} \tag{57}$$

(see [16] for a discussion of energy methods). We have restricted the analysis to passive models, (8), so by letting $\eta > \epsilon > 0$, we get an L^2 bound of the fields. Now, let $\hat{p}_1$ and $\hat{\boldsymbol{v}}_1$ be the difference between the solution to the dispersive model, (12), and the non-dispersive model, (11). The difference fields satisfy

$$\begin{aligned} &s\kappa\hat{p}_1 + \nabla\cdot\hat{\boldsymbol{v}}_1 = s(\kappa(s)-\kappa)\hat{p} \\ &s\rho\hat{\boldsymbol{v}}_1 + \nabla\hat{p}_1 = \mathbf{0}. \end{aligned} \tag{58}$$

We use the special structure of the approximate dispersive model (12) and the energy estimate (57) to get the bound

$$\kappa_0\|\hat{p}_1\|_3^2 + \rho_0\|\hat{\boldsymbol{v}}_1\|_3^2 \leqslant C_{\mathrm{a}}\frac{|s|^6\kappa_0\|\hat{p}\|_3^2}{|\omega_0^2+s^2|^2\epsilon(\eta-\epsilon)} \tag{59}$$

where the constant C_{a} only depends on the medium parameters. For large values of the approximation parameter ω_0, the error fields vanish, i.e.

$$\hat{p}_1 \to 0 \qquad \text{and} \qquad \hat{\boldsymbol{v}}_1 \to 0 \qquad \text{in} \quad \mathrm{L}^2(\mathbb{R}^3). \tag{60}$$

For the time-domain convergence, we use the frequency-filtered fields in (13). The frequency-filtered time-domain fields $p_1(t)$ and $\boldsymbol{v}_1(t)$ are bounded as

$$\begin{aligned} \left(\int_0^T \kappa_0\left\|\int_{-\infty}^{\infty}\mathrm{e}^{st}\hat{p}_1(s)\hat{\chi}_{\omega_{\mathrm{m}}}(s)\,\mathrm{d}\omega\right\|_3^2\mathrm{d}t\right)^{1/2} &\leqslant C_{\mathrm{b}}\int_{-\infty}^{\infty}\|\hat{p}_1(s)\|_3|\hat{\chi}_{\omega_{\mathrm{m}}}(s)|\,\mathrm{d}\omega \\ &\leqslant C_{\mathrm{c}}\int_{-\infty}^{\infty}\left|\frac{s^3\hat{\chi}_{\omega_{\mathrm{m}}}(s)}{\omega_0^2+s^2}\right|\mathrm{d}\omega \leqslant C_{\mathrm{d}}\omega_0^{-1} \end{aligned} \tag{61}$$

where the constant C_{d} only depends on η, T, ω_{m} and the norm of the sources. The last inequality in (61) follows from the decay of the weight function (14). Hence, the smoothed dispersive fields $\tilde{p}_{\omega_0}(t)$ and $\tilde{\boldsymbol{v}}_{\omega_0}(t)$ approach the non-dispersive fields $\tilde{p}(t)$ and $\tilde{\boldsymbol{v}}(t)$ as $\omega_0 \to \infty$.

References

[1] Atkinson F V 1960 Wave propagation and the Bremmer series *J. Math. Anal. Appl.* **1** 255–76

[2] Bremmer H 1951 The W.K.B. approximation as the first term of a geometric-optical series *Commun. Pure Appl. Math.* **4** 105–15

[3] Colton D and Kress R 1983 *Integral Equation Methods in Scattering Theory* (New York: Wiley)

[4] Corones J P 1975 Bremmer series that correct parabolic approximations *J. Math. Anal. Appl.* **50** 361–72

[5] de Hoop M V 1996 Generalization of the Bremmer coupling series *J. Math. Phys.* **37** 3246–82

[6] de Hoop M V and Gautesen A K 1999 Uniform asymptotic expansion of the generalized Bremmer series *SIAM J. Appl. Math.* at press

[7] Fishman L 1992 Exact and operator rational approximate solutions of the helmholtz, weyl composition equation in underwater acoustics—the quadratic profile *J. Math. Phys.* **33** 1887–914

[8] Fishman L, de Hoop M V and van Stralen M J N 1999 Exact constructions of Helmholtz operator symbols the focusing quadratic profile *J. Math. Phys.* submitted

[9] Fishman L, Gautesen A K and Sun Z 1997 Uniform high-frequency approximations of the square root Helmholtz operator symbol *Wave Motion* **26** 127–61

[10] Graves R W and Clayton R W 1990 Modelling acoustic waves with paraxial extrapolators *Geophysics* **55** 306–19

[11] He S, Ström S and Weston V H 1998 *Time Domain Wave-Splittings and Inverse Problems* (Oxford: Oxford University Press)

[12] Hörmander L 1985 *The Analysis of Linear Partial Differential Operators* vol 3 Grundlehren der mathematischen Wissenschaften vol 256 (Berlin: Springer)

[13] Ishimaru A 1991 *Electromagnetic Wave Propagation, Radiation, and Scattering* (Englewood Cliffs, NJ: Prentice-Hall)

[14] Keller H B and Keller J B 1962 Exponential-like solutions of systems of linear ordinary differential equations *J. SIAM* **10** 246–59

[15] Keller J B and Papadakis J S (ed) 1977 *Wave Propagation and Underwater Acoustics* (Berlin: Springer)

[16] Kreiss H-O and Lorenz J 1989 *Initial-Boundary Value Problems and the Navier–Stokes Equations* (San Diego: Academic)

[17] Lee D and Pierce A D 1995 Parabolic equation development in recent decade *J. Comput. Acoustics* **3** 95–173

[18] McMaken H 1986 On the convergence of the Bremmer series for the Helmholtz equation in 2-D *Wave Motion* **8** 277–83

[19] Strikwerda J C 1989 *Finite Difference Schemes and Partial Differential Equations* (New York: Chapman and Hall)

[20] van Stralen M 1997 Directional decomposition of electromagnetic and acoustic wave-fields *PhD Thesis* Delft University of Technology